

OPEN ACCESS

EDITED BY
Rochelle Diane Seitz,
College of William & Mary, United States

REVIEWED BY
Valentina Asnaghi,
University of Genoa, Italy
Hairong Wang,
Carnegie Mellon University Stores,
United States

*CORRESPONDENCE
Victoria G. Mason
Victoria.mason@nioz.nl

[†]These authors have contributed equally to this work and share first authorship

RECEIVED 07 July 2025 ACCEPTED 08 September 2025 PUBLISHED 01 October 2025

CITATION

Mason VG, van Leeuwe J, Bouma TJ, Sinke D, Varley D, Heide Tvd, Temmink RJM, Bucher F and van Belzen J (2025) Using local materials for scalable marine restoration: Xiriton as a nature-enriching, low impact building material. *Front. Mar. Sci.* 12:1661288. doi: 10.3389/fmars.2025.1661288

COPYRIGHT

© 2025 Mason, van Leeuwe, Bouma, Sinke, Varley, Heide, Temmink, Bucher and van Belzen. This is an open-access article distributed under the terms of the Creative Commons Attribution License (CC BY). The use, distribution or reproduction in other forums is permitted, provided the original author(s) and the copyright owner(s) are credited and that the original publication in this journal is cited, in accordance with accepted academic practice. No use, distribution or reproduction is permitted which does not comply with these terms.

Using local materials for scalable marine restoration: Xiriton as a nature-enriching, low impact building material

Victoria G. Mason^{1,2*†}, Jente van Leeuwe^{1,3†}, Tjeerd J. Bouma^{1,2}, Dagmar Sinke^{1,4}, Daniel Varley^{5,6}, Tjisse van der Heide^{5,6}, Ralph J. M. Temmink⁷, Frank Bucher⁸ and Jim van Belzen^{1,9}

¹Department of Estuarine and Delta Systems, Royal Netherlands Institute for Sea Research, Yerseke, Netherlands, ²Department of Physical Geography, Faculty of Geosciences, Utrecht University, Utrecht, Netherlands, ³Aquatic Ecology and Water Quality Management Group, Wageningen University & Research, Wageningen, Netherlands, ⁴HZ University of Applied Sciences, Vlissingen, Netherlands, ⁵Department of Coastal Systems, Royal Netherlands Institute for Sea Research, Den Burg, Netherlands, ⁶Conservation Ecology Group, Groningen Institute for Evolutionary Life Sciences, University of Groningen, Groningen, Netherlands, ⁷Copernicus Institute of Sustainable Development, Utrecht University, Utrecht, Netherlands, ⁸Independent Researcher, Leeuwarden, Netherlands, ⁹Wageningen Marine Research, Wageningen University & Research, Yerseke, Netherlands

Materials currently used to produce reef structures are often limited by high production costs, negative environmental impacts or limited flexibility in design and degradability. We tested the ability of a novel concrete alternative, Xiriton, to i) exhibit adjustable erodibility using different mixtures, ii) limit the input of foreign products into the marine environment by using locally sourced building materials (e.g. local C4 grass Spartina anglica or Miscanthus giganteus, crushed shells and sand) and iii) facilitate the establishment of marine organisms. In addition to material testing of compressive strength, porosity and pH, we combined direct measurements of erosion in a fast flow flume with field measurements of erosion over time at different heights in the intertidal frame. Furthermore, we monitored the settlement of marine organisms onto Xiriton blocks placed into the field. We showed that i) while the erodibility of Xiriton can be made comparable with more conventional building materials, its degradability can be easily adjusted by altering the proportion of binding material in the mixture, ii) the use of locally sourced building materials did not reduce the structural integrity of the material but did minimise its potential long-term impacts on the environment, and that iii) Xiriton acts as a colonisable building material by facilitating the rapid establishment of species such as seaweeds, barnacles, Pacific oysters and blue mussels, and thus may enhance biodiversity. While further research is necessary to understand the longer-term behaviour and impacts of Xiriton, its simple production process, minimal short-term impacts and adjustable erodibility reveal a strong potential for its application in marine restoration using local ingredients on a global scale.

KEYWORDS

artificial reefs, living shorelines, coastal defence, environmental impact, nature-based solutions, saltmarsh

1 Introduction

With 2.15 billion people currently living in the near-coastal zone, and this number expected to rise to 2.9 billion across the 21st century (Reimann et al., 2023), the need for resilient coastlines is of growing importance. Currently, to protect coastlines, an estimated US\$ 12-71 billion annually is spent on dike investment and maintenance worldwide (Hinkel et al., 2014). Climate change driven impacts including sea level rise and increasing frequency of extreme weather events present additional threats to coastal areas (Bouma et al., 2014; Leonardi et al., 2016; Saintilan et al., 2022). Traditionally, coastlines have been protected from flooding with hard defences, such as dikes and seawalls (Zhu et al., 2020). Recently however, coastal ecosystems such as vegetated wetlands and shellfish reefs have been promoted for the role they can play within flood defence strategies as 'Nature-based Solutions' (NbS); either alone as 'green' solutions or in combination with hard defences as 'green-grey' solutions (Gedan et al., 2011; Shepard et al., 2011; Temmerman et al., 2013; Narayan et al., 2016; Schoonees et al., 2019). Such ecosystems bring with them myriad services, such as carbon storage (Davis et al., 2015; Temmink et al., 2023; Mason et al., 2023) and enhanced biodiversity (Morris et al., 2022), while having the potential to adapt to changing circumstances such as sea-level rise (Kirwan and Megonigal, 2013).

When implementing NbS, it can be necessary to use humanmade structures to i) protect the extent of existing coastal ecosystems (Marin-Diaz et al., 2021), ii) facilitate the establishment of protective shellfish reefs (Howie and Bishop, 2021), and/or iii) create windows of opportunity to enable vegetation establishment (Sakr and Altieri, 2025). In the first case (i), where land constraints for example limit dike raising/widening, a saltmarsh in front of the dike may be incorporated into flood defence planning (Marin-Diaz et al., 2023). A wider marsh can attenuate more waves via its raised bed elevation and vegetation drag (Möller et al., 2014; Vuik et al., 2016; Zhu et al., 2020; Marin-Diaz et al., 2023). Where erosion prevention is required to maintain a sufficient cross-shore width for wave attenuation (Vuik et al., 2016; Zhu et al., 2020), or where marsh erosion becomes persistent due to climate-change driven erosion (Campbell et al., 2022), there may be a need to protect the marsh edge to maintain its width by placing structures to reduce hydrodynamic forcing and stimulate sediment deposition, thus slowing lateral erosion (Van Loon-Steensma and Vellinga, 2013). In the second case (ii), humanmade structures may be placed on the coastline to stimulate the formation of shellfish reefs, where hydrodynamic conditions are suitable for larvae to settle (Theuerkauf et al., 2015; Walles et al., 2016; Fivash et al., 2021). The stimulation of reef formation may provide a way to directly protect intertidal zones and coastlines (Borsje et al., 2011; Smith et al., 2020; Fivash et al., 2021) or may be relevant in more 'seascape scale' coastal defence, in which multiple ecosystems and their interactions are incorporated (Chowdhury et al., 2019; Schoonees et al., 2019; Howie and Bishop, 2021). Established reefs in front of a saltmarsh edge could attenuate waves to reduce saltmarsh erosion, which would in turn maintain greater wave attenuation capacity of the saltmarsh in front of the dike (Bouma et al., 2014; van de Koppel et al., 2015). Artificial reef structures can be used for this purpose (Marin-Diaz et al., 2021) but could also be used as scaffolding, facilitating only the initial formation with the longer-term objective of a natural, selfsustaining reef (Piazza et al., 2005; Walles et al., 2016; Bersoza Hernández et al., 2018; Fivash et al., 2021; Pan et al., 2022). Building materials used for artificial reefs should therefore ideally have adjustable erodibility to account for different timescales of reef formation, and a structure which encourages the settlement of bivalve larvae (Bersoza Hernández et al., 2018). Similarly, in the third case (iii), structures with adjustable erodibility may be ideal for creating short-lived windows of opportunity that reduce waves and sediment-dynamics, which are crucial for seedling establishment and subsequent survival (Balke et al., 2011, 2014, Bouma et al., 2016; Cao et al., 2020). In this case, the structures should be designed to last only until the target species is established and self-sustaining. The structure and lifespan of materials should also be adjustable according to the local environmental conditions in which they are deployed. For example, structures might need to be adapted for different emergence or inundation times in microtidal compared to macrotidal systems or should be designed to have a higher erosion resistance in areas exposed to strong wind-waves or tidal currents.

Currently, several materials are used to protect intertidal areas or to create habitat providing structures (bioreefs) (Barausse et al., 2015; Marin-Diaz et al., 2021). Rocks, concrete-like materials, traditional (persistent) or biodegradable plastics, sandbags and wood are among the materials frequently used to build protective structures (Green et al., 2012; Smith et al., 2020; Marin-Diaz et al., 2021; Polk et al., 2022). Each of them has benefits and limitations (briefly outlined in Table 1) in terms of feasibility, environmental impact, shapeability and adjustability of lifetime:

- 1. Feasibility: rocks, wood, sandbags and concrete are easy to obtain in large quantities and therefore cheap and fast to deploy. However, biodegradable plastic alternatives, such as BESE-elements® (Marin-Diaz et al., 2021),) can be more challenging to produce and can be more expensive (Nitsch et al., 2021). Currently, they are often more viable for smaller-scale projects. Such feasibility, or lack thereof, is crucial to the potential for upscaling material deployment to larger projects or a greater range of locations.
- 2. Environmental impact: traditional plastics are slow to break down and remain in the environment over long timescales; more recently, biodegradable plastics used in coastal structures are generally designed to breakdown within decades, or over very short timescales (Nitsch et al., 2021; Comba et al., 2023), although the exact lifetime may vary in different environmental settings. The same is applicable for geotextile casings of geotextile filled sand containers, although sand itself has a limited impact (Corbella and Stretch, 2012). Wood tends to have a low environmental impact in terms of waste products (Dickson et al., 2023). In contrast, both rocks (Wijsman et al., 2024) and concrete (Hillier et al., 1999) pose the risk of leaching heavy metals into the surrounding environment. Concrete and similar

Mason et al.

TABLE 1 Suitability of materials currently used to build protective structures in marine and/or intertidal environments: rocks, concrete, traditional plastics, bioplastics, wood and sandbanks.

Material	Feasibility	Environmental impact	Shapeability	Lifetime control	Example
Rocks	High; cheap and easy to obtain.	Intermediate; potential heavy metal leaching.	Low; difficult to adjust shape/size.	Low; non-adjustable breakdown time.	Nordstrom (2014)
Concrete	High; cheap and easy to obtain.	High; potential heavy metal leaching or alkalinity changes.	High; can be moulded into different structures.	Low; non-adjustable breakdown time.	Nordstrom (2014)
Traditional (persistent) plastics	High; cheap and easy to obtain.	High; e.g. potential leaching into seawater.	High; can be produced in different structures/densities.	Low; typically long breakdown time.	Ashis (2015)
Biodegradable plastics (e.g. BESE-elements®)	Low; expensive, more difficult to source.	Low; often designed for minimal leaching.	High; can be produced in different structures/densities.	Intermediate; various breakdown times being developed but still often unpredictable.	March 2017 Deployment + Monitoring Marin-Diaz et al. (2021)

Material	Feasibility	Environmental impact	Shapeability	Lifetime control	Example
Wood (e.g. brushwood dams)	High; cheap and easy to obtain.	Low; use of natural materials limits impact.	Low; size may be adjustable but shape difficult to adjust.	Low; non-adjustable breakdown time.	Photo taken by V. Mason at Holwert, NL in October 2024
Sandbags (e.g. Geotextile sand filled containers)	High; cheap and easy to obtain.	Intermediate; dependent on geotextile properties and sand extraction.	Low; size of overall structure may be adjustable but shape difficult to adjust.	Low; non-adjustable breakdown time.	Corbella and Stretch (2012)

Each material is assessed in terms of feasibility, environmental impact, shapeability and lifetime control, with positive properties shown in green, negative properties shown in red and moderately negative properties shown in yellow. These rankings are based on literature outlined in 1.0 Introduction. Examples show applications of each material in the field as given in previously published literature.

alternatives may also increase the alkalinity in their direct vicinity (Setunge et al., 2009), altering which species can successfully establish. Furthermore, the industrial process required to produce concrete is energetically expensive and is responsible for large CO₂ emissions (Achternbosch et al., 2011). Such impacts of concrete vary by composition and have been alleviated in some newer developed materials, such as ECOncrete[®] Antifers, which have been developed with more similar surface pH to seawater and thus minimal pH effect (Ido and Shimrit, 2015).

- 3. Shapeability: a benefit of biodegradable plastics and concrete structures is the possibility to shape them to adjust their suitability for specific uses, for instance, structures designed to provide habitat for species settlement. Rock and wooden structures are less easily shaped, making them more suitable for obstruction constructions, like (brushwood) dams and groynes (Nordstrom, 2014). Adapting shapes and designs to mimic emergent traits of the ecosystem being restored or protected has been shown to increase the chance of restoration success (Temmink et al., 2023).
- 4. Lifetime: for conventionally used materials, lifetime may be difficult to control, while newer materials often have largely unknown lifetimes, in both cases making it more difficult to fit the lifetime-construction to the needs of an environment. For instance, concrete can last more than fifty years in intertidal environments and rocks almost forever, while establishment of bivalve, and specifically oyster, reefs generally only takes up to 5 years (Morris et al., 2022). Removal of constructions following reef formation could be harmful for established ecosystems and could introduce substantial additional costs (Nordstrom, 2014).

Each material may be better suited to specific scenarios. For example, brushwood is ideal for simple-shaped dams where the priority is to use readily available and natural materials. Bioplastics, on the other hand, are well-suited to smaller-scale projects where cost is less of a constraint and flexibility in shape is a key requirement. However, given the limitations of conventional materials (Table 1), there is a need to develop new, sustainable materials for artificial reef construction that combine a high feasibility, low environmental impact, high shapeability and adjustable lifetime. To this end, a novel hydraulic concrete alternative called Xiriton was investigated. Developed by Bucher (2022), Xiriton is a low-emission, concrete-like material that can be produced primarily using components naturally found in coastal areas. Xiriton can overcome various key limitations of other materials: (1) it is made via a simple mixing process using easily available and cheap materials; (2) naturally occurring seawater and local ingredients can be used to limit environmental impact; (3) the shape and durability of Xiriton can be easily adjusted via different moulds and mixtures. These three properties allow Xiriton to be designed with lifetimes that meet the needs of specific projects, and which can be easily upscaled. Xiriton shows potential for application as a coastal engineering material both to directly protect coastal defences or ecosystems and to stimulate the formation of shellfish reefs. The fibres of Xiriton originate from locally sourced C4 grasses, such as Miscanthus giganteus (Elephant grass) or Spartina anglica (Common Cordgrass). Both grasses are locally widely available in the Netherlands and have similar C4 equivalents occurring in other countries around the world, indicating that Xiriton production could be upscaled across more locations. Using Spartina anglica, a saltmarsh grass, for intertidal restoration can help ensure that only locally occurring species are introduced into the environment if the Xiriton material degrades. While similar concepts can be applied across different regions globally by using local species, it may be beneficial to find multiple species as an ingredient for Xiriton to prevent the overharvesting of a single species. For example, Spartina anglica and other saltmarsh vegetation species play an important role in sediment stabilisation via their roots and wave attenuation via their stems (see e.g. Ysebaert et al., 2011) and should not be indiscriminately harvested. As Xiriton is a newly developed material, its properties and effectiveness as a nature-enriching building material remain unknown, requiring rigorous testing before large-scale application.

Here, we aimed to assess the applicability of Xiriton as an alternative nature-enriching material for NbS by creating Xiriton with a range of shapes and varying compositions of marine-sourced raw materials, by testing for the following key characteristics: i) erodibility, ii) compressive strength, iii) porosity, iv) pH, and v) establishment of marine organisms. Erosion of Xiriton blocks was compared with that of other novel hydraulic materials under raised hydrodynamic conditions in a fast flow flume. Furthermore, erosion of Xiriton blocks with varying compositions of marine-sourced raw materials and drying times was compared in the fast flow flume (rapid short-term erosion) and in-situ on an intertidal flat in a mesotidal environment ('real time' erosion). Additional material testing was carried out to compare the compressive strength, porosity and pH of different mixtures. Establishment of marine organisms on Xiriton blocks on the intertidal flat was also recorded over time. In doing so, we provided insight into the adjustability of erodibility of Xiriton mixtures alongside the potential for reef establishment. Gaining insight into each of these processes will contribute to the development and potential application of Xiriton within coastal engineering projects and NbS.

2 Materials and methods

2.1 Experimental design and Xiriton tests

Xiriton does not use Portland cement in the manufacturing procedure and uses plant material, thereby decreasing its carbon footprint (Bucher, 2022). Xiriton is generally made from four components: 1) a type of C4 grass (providing structure and replacing reinforcing steel in conventional concrete) 2) a combination of volcanic pozzolan and slaked lime (to act as binding materials) 3) fresh or seawater and 4) optional additives

such as shells (to adjust the material properties) (Bucher, 2022). In this research, *Spartina anglica*, a common saltmarsh species in the Netherlands and NW Europe, and *Miscanthus* giganteus, or Elephant grass, were used as the C4 grass. Through the experiments described in this study, we aimed to produce Xiriton in a range of shapes, sizes and compositions.

The testing of Xiriton was divided into three stages (Supplementary Figure S1):

- Comparison of Xiriton (XS5S-N4 mixture) with other alternative building materials
 - i. Erosion measurements under controlled flume conditions (fast flow flume).
- 2. Comparison of Xiriton recipe variations to regulate erodibility
 - i. Measurements: compressive strength, porosity and pH.
 - Erosion measurements under controlled flume conditions (fast flow flume).
 - iii. Erosion measurements in a field setting under intertidal conditions.
- 3. Comparison of Xiriton recipe for establishment of marine organisms onto Xiriton structures
 - Observations of establishment of marine organisms onto Xiriton structures in intertidal field conditions.

2.2 Recipes for creating Xiriton mixtures and comparison materials

For the first stage (1 - erodibility Xiriton vs. other Portland cement alternatives), a baseline Xiriton mixture 'XS5S-N4' was produced using Tubag TK traskalk (55% pozzolan, 45% slaked lime), Spartina anglica cuttings, crushed oyster shells (0-8mm) and seawater. This was compared with more 'conventional' and varied building materials, which avoided the use of Portland cement: non-Portland, non-Portland: strengthened, and non-Portland: coconut fibre. In each conventional material, Roman cement (De Mortel Compagnie, https://kalkshop.nl/product/romeins-cement/) was used in place of Portland cement to avoid quick-hardening agents and to produce potentially erodible concretes. The mixtures of each material are outlined in Table 2. The volcanic pozzolan consisted mostly of silicic acid (SiO₂) and reactive alumina (Al₂O₃) (Ghahari et al., 2017). When this is mixed with water and lime $(Ca(OH)_2)$ it reacts to create solid calcium silicates (C - S - H) and calcium aluminate hydrates (C - A - H) (Dunstan, 2011; Indrawati and Manaf, 2008). Once poured, the concrete bricks were kept under a wet cloth for one week before being stored in a room temperature environment for another three weeks. The blocks of all materials were poured into a conventional 'brick' type shape (0.395m (length) x 0.1m (width) x 0.06m (depth) (Figure 1A).

For the second stage (2 – regulating erodibility Xiriton), four contrasting Xiriton mixtures were produced with increasing quantities of volcanic pozzolan and slaked lime, to strengthen the material and increase the predicted lifetime (Table 2), along with unfiltered seawater from the Oosterschelde (30 ppt), Common Cordgrass (Spartina anglica), and sand and shells (additives). Spartina anglica was gathered from a saltmarsh in the Oosterschelde (the Netherlands) at Rattekaai (51°26'17.2"N, 4° 09'59.1"E) 13 days before pouring the mixtures, then dried on newspaper in a dry greenhouse for 14 days and cut into 1-3cm long straws. This was used to provide structure to the mixtures. The added shell mixture contained crushed shells with sizes varying from completely crushed up to 2cm pieces, to allow some heterogeneity within the mixture. The four mixtures (N5a-d) were moulded into tapering cylindrical blocks to allow flow and subsequent erosion to occur around each sample in the flume (diameter at base = 0.07m, diameter at top = 0.045m, height = 0.09m) (Figure 1B). Each block had a volume of approximately 0.2L. This size was chosen to allow the flow of water around each side of the blocks in the fast flow flume once secured in an inverted position to the test section.

Finally, for the third stage (3 – settlement on Xiriton), three replicate Xiriton blocks were produced with the following dimensions: 0.30m x 0.30m x 0.20m (Figure 1A). These blocks were made up of the same mixture as XS5S-N5b but using *Miscanthus giganteus* replacing *Spartina anglica* as fibres to provide structure (Table 2).

2.3 Comparison of Xiriton with other building materials (stage 1 - testing)

During stage 1 of testing, erosion of Xiriton was tested in comparison to other alternative coastal building materials under controlled flume conditions. The flume experiments took place in a 'fast flow flume' (Figure 2; see Marin-Diaz et al. (2022); Stoorvogel et al. (2024)) designed to simulate high velocity hydrodynamic events. The flume setup consisted of three fast flow flumes, each with a water reservoir and four slots into which samples could be placed. Due to a constant refilling rate (247 L min⁻¹) of the water reservoir, the water velocity in the flume in an equilibrium state was determined by the water height in the reservoir and the opening height of the sluice gate (h_0 and h_1 in Figure 2, respectively).

Using the method of Marin-Diaz et al. (2022), but with an updated version of the flume as described in Stoorvogel et al. (2024), the discharge was calculated by relating the water velocity to h_2 (the water height over the eroding object (Equation 1)):

$$d = h_0 h_2 \left(\frac{2g}{h_2 + h_0}\right)^{0.5} \tag{1}$$

Where d = discharge (m² s⁻¹), h_0 = height water column tank (m; Figure 2); h_1 = height opening tank (m; Figure 2); g = earth gravitational acceleration (9.81 m s⁻²) and h_2 = the water height over the eroding object (m; Figure 2). The value of h_2 was calculated as (Equation 2):

$$h_2 = h_1/c_{contract}, (2)$$

TABLE 2 Xiriton building components for each of the 6 mixtures created across the three testing stages, with the volume fraction of each component per mixture.

Testing stage	Recipe	Fiber (S = <i>S. anglica</i> ; C = Coconut; M = <i>Miscanthus</i>)	Mixed shells (O = Only Oyster shells)	Sand	Pozzolan (T = Trass)	Roman cement	Slaked lime	Water (S = seawater; F = Fresh water)
	Units	m ³	m ³	m ³	m ³	m ³	m ³	m ³
1 Erodibility Xiriton vs. conventional	Xiriton mix XS5S-N4	5 (S)	3 (O)		1.65 (T)		1.35	3 (S)
	Non-Portland		0.8	0.8	1 (T)	0.3	2.7	0.72 (F)
	Non-Portland: strengthened		0.75	0.75	1 (T)	0.2	1.8	0.56 (F)
	Non-Portland: coconut fibres	0.4 (C)	0.8	0.8	1 (T)	0.3	2.7	0.72 (F)
2 Regulating erodibility of Xiriton	Xiriton mix XS5S-N5a	4 (S)	2	2	1		0.5	3 (S)
	Xiriton mix XS5S-N5b	4 (S)	2	1	2		1	3 (S)
	Xiriton mix XS5S-N5c	4 (S)	3	0	3		1	3 (S)
	Xiriton mix XS5S-N5d	4 (S)	4	0	3		3	3 (S)
3 Settlement	Xiriton mix XM5S-N5b	4 (M)	2	2	1		0.5	3 (S)

^{&#}x27;XS' refers to Xiriton using Spartina or 'XM' to Xiriton using Miscanthus, '55' refers to the use of pozzolan, slaked lime and crushed shells, and 'Nx-x' refers to the mixture identifier. The testing stage refers to the objective for which the mixtures were used: Stage 1: Comparison of Xiriton with conventional and other alternative building materials; Stage 2: Comparison of Xiriton recipe variations to regulate erodibility); and Stage 3: Observations of establishment of marine organisms onto Xiriton structures in intertidal field conditions.

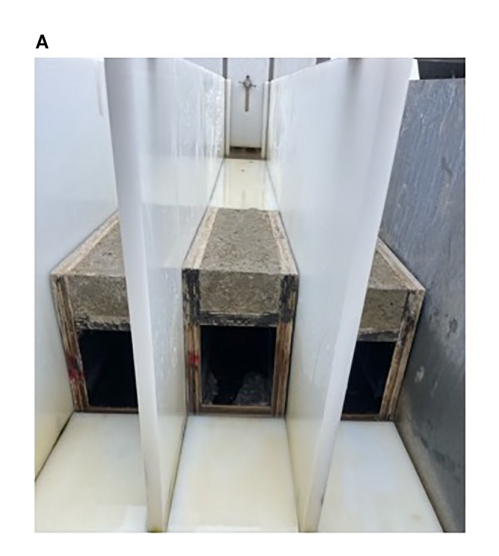




FIGURE 1
Photographs of the material shapes used in the fast flow flume. (A) The bricks used for the erosion experiment of Xiriton compared to other alternative coastal engineering materials. (B) The cylindrical blocks used for the erosion experiments with various Xiriton recipes in the fast flow flume and in the field. Photos taken by V. Mason and (J) van Leeuwe.

with $c_{contract}$ being a contraction constant of 0.6 (-) taken from Marin-Diaz et al. (2022). The water velocity (u; m s⁻¹) was subsequently calculated as (Equation 3):

$$u = d/h_2 \tag{3}$$

Bricks of the i) Xiriton (XS5S-N4), ii) non-Portland, iii) non-Portland: strengthened, and iv) non-Portland: coconut fibre mixtures were placed into each slot of the fast flow flume, giving a total of 4 types of bricks for comparison. Bricks were arranged in a random distribution in each flume (12 in total), i.e. 4 treatments each with three replicates (n = 3). The bricks were then subjected to a flow velocity of approximately 4.5 m s⁻¹ for a total duration of 63 days. Vertical erosion (cm) was measured using an erosion bar setup at 0 hours, 3 hours, 24 hours, 48 hours, 72 hours, 96 hours, 14 days, 21 days, 28 days, 35 days, 42 days and 63 days after test start. Measurements were taken at 10 points each on duplicate transects across each block.

2.4 Comparison of Xiriton recipe variations to regulate erodibility (stage 2 - testing)

2.4.1 Experimental measurements: compressive strength, porosity and pH

To compare the material properties of each Xiriton mixture used in stage 2 (see Table 2), compressive strength was measured using an Instron EMSYSL7049 Universal Testing Machine, following the method in the ASTM International Committee C09 on Concrete and Concrete Aggregates (ASTM International Subcomittee C09.61, 2014). In accordance with this method, each block was compressed at a speed of 50mm min⁻¹ using a 5kN loading cell (standard concrete testing procedures) until the load of failure pressure was reached. Each mixture and curing period (the time between the pouring and the deployment of the material in which the material can harden) was measured with triplicate blocks. Compressive strength was calculated as (Equation 4):

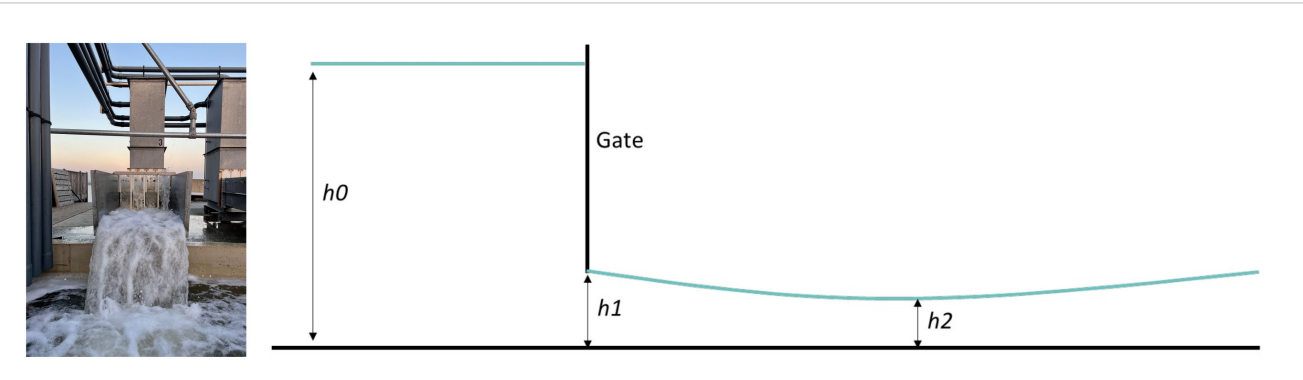


FIGURE 2
Photograph of the fast flow flume and schematic fast flow flume profile (from Marin-Diaz et al. (2022). h_0 represents the water level in the reservoir, seen as the tower in the photograph. h_1 represents the height of the gate and h_2 is the water height in the flume calculated from h_1 . Photo taken by V. Mason.

Compressive strength(MPa)

= Load to failure(N)/cross sectional area(
$$m^2$$
) (4)

and rounded to the nearest 0.1MPa.

Following erodibility measurements, porosity and pH measurements were taken for mixtures N5b, N5c and N5d, since the N5a samples had been fully eroded during testing. Twelve sample blocks of each mixture were taken for testing, with all 12 blocks sampled for initial porosity and pH, and 4 replicate blocks sampled for pH change with 1-, 2- or 5-weeks submersion in seawater. The blocks were fully dry prior to submersion following several months of storage in dry conditions. Each block was weighed individually both before and immediately after submersion to measure porosity (%), which was calculated as (Equation 5):

Porosity(%)

=
$$(\text{Wet weight}(g) - \text{dry weight}(g))/\text{wet weight}(g) * 100.$$
 (5)

To measure initial pH, each sample was gently sanded and the resulting powder sieved (1mm mesh size). Five grams of the sieved powder were placed into a sample bottle, to which 25ml of KCl solution (74.56g KCl:1L distilled water) was added. The sample bottle was shaken and stirred using a magnetic stirrer. A calibrated Metrohm 713 pH meter was then placed into the sample for 2 minutes and a pH reading was taken. The sensor was cleaned with distilled water in between measurements to prevent contamination. Four replicates of each mixture were fully submerged in covered plastic tanks of seawater (salinity = 30 ppt) for 1-, 2- or 5-weeks. Following submersion, each sample was allowed to fully dry for approximately 2 weeks, before the above process was repeated to remeasure pH.

2.4.2 Erosion measurements under controlled flume conditions

For the erosion tests of stage 2, Xiriton samples of different mixtures and curing times (Table 2) were produced in small, tapering cylindrical blocks (volume = 0.2L) so that four samples could be placed into each slot of the fast flow flume. The position of the mixtures was varied between each slot to account for the effect of sheltering on erosion (Figure 1). Three flumes allowed for three replicates of each measurement. Each block was placed upright so it would be hit frontally by the water flow, and to allow flow around the blocks during a 24-hour run period. Each block was weighed before the experiment, both dry and after 24-hour submergence in seawater. Erosion was compared between different curing times, using one flow velocity (3.5 m s⁻¹). Erosion was also compared between different flow velocities (1.5, 2.5, 3.5 and 4.5 m s⁻¹), using mixtures of one curing, or drying, time (5 weeks). The order of each velocity test was randomised to account for possible differences in curing time between the first and last mixtures tested.

Each block was weighed after 0 minutes, 1 hour, 2 hours, 5 hours and 24 hours (total run time) in the flume experiment. The starting volume of each block was approximated from the volume of the control blocks, and end volume was measured (except for the

N5a samples which had eroded completely) after the flume tests, using a simple water displacement measurement.

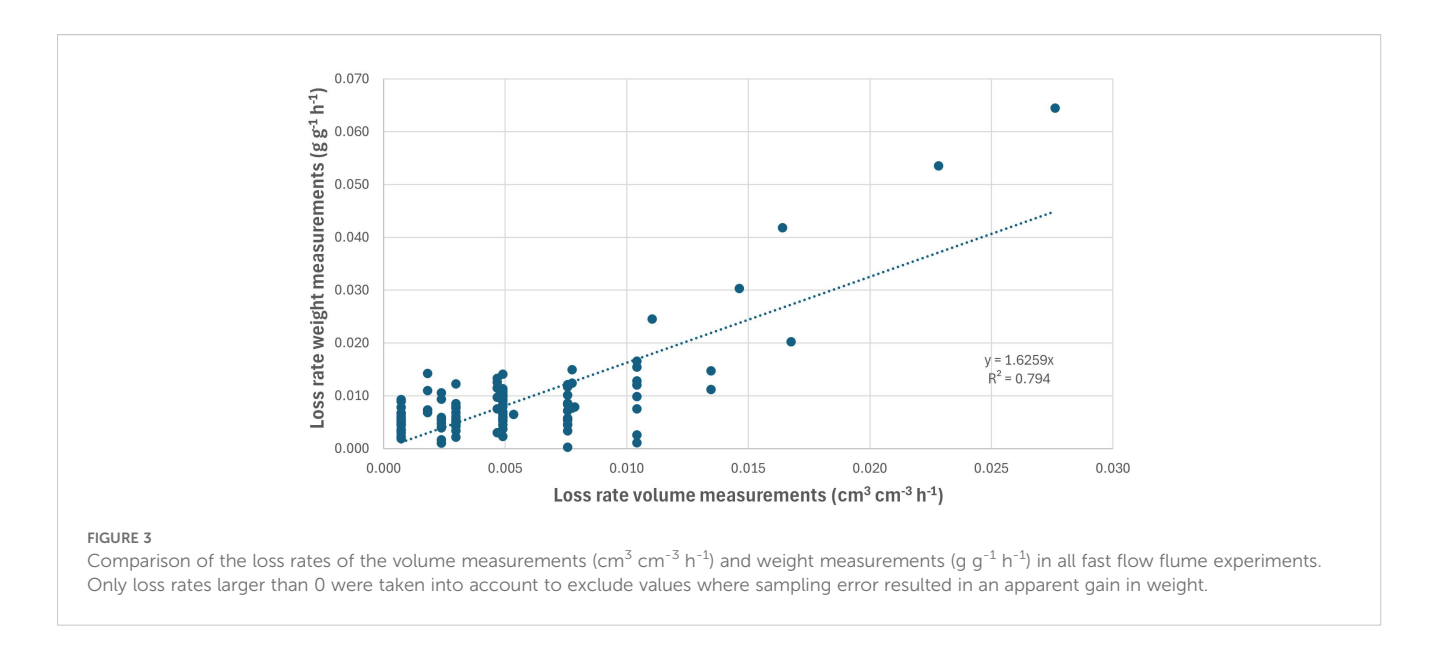
2.4.3 Erosion measurements under intertidal conditions

Erosion of contrasting Xiriton mixtures was also measured under field conditions, by placing samples onto a mudflat, near Yerseke (51°29'20.0"N, 4°03'28.0"E), SW Netherlands, for 5 weeks in March-April 2024. This area is an intertidal mudflat adjacent to the Royal Netherlands Institute for Sea Research (NIOZ) in the Oosterschelde estuary, with a salinity of approximately 30 ppt and a tidal range of approximately 2.5-3.5m (de Vet et al., 2017). Xiriton blocks were attached to a frame at 2 heights above the bed (0m and 1.42m), with a bed level of -0.95 ± 0.02 m+NAP (Normaal Amsterdams Peil), resulting in different inundation periods during the tidal cycle. Three blocks of each mixture were attached at each height, again in a random order to account for possible sheltering. An OSSI wave gauge OSSI-010-003C was placed close to the field set-up to measure water level (m) and significant wave height (m) across the measurement period, which were later used to calculate bed shear stress. The wave gauge was set at a measurement interval of 15 minutes, with measurement periods of 7 minutes at a 5 Hz frequency.

In the field experiment, erosion of contrasting Xiriton blocks was initially measured by weekly weighing. However, this method proved logistically challenging due to variations in emergence time after high tide, leading to inconsistent water content between measurements and potential errors. Drying the blocks to a consistent water content would have required removing them from the field, potentially interfering with treatment conditions. Therefore, block volume change was used as an alternative measure of erosion. Given that the initial volume of each block was known, final volumes were determined using the water displacement measurements, as described above. To enable comparison between the field and flume experiment, a correlation was established between weight and volume measurements in the flume. This relationship allowed volume-based erosion in the field to be translated into weight-based erosion, comparable to the flume measurements (Figure 3). Despite some variability in lower values, the correlation between weight and volume was significant.

2.5 Establishment of marine organisms onto Xiriton structures (stage 3 - testing)

During stage 3 of testing, three replicate blocks of Xiriton (dimensions: $0.30 \,\mathrm{m} \times 0.30 \,\mathrm{m} \times 0.20 \,\mathrm{m}$) were placed onto an intertidal flat in the Eastern Scheldt at an elevation of approximately $-0.64 \pm 0.02 \,\mathrm{m} + \mathrm{NAP}$ in November 2023. The blocks were left for a 12-month period and regularly checked for erosion or settlement of marine organisms. In November 2024, each block was photographed and checked for erosion, as well as settlement of organisms such as brown and green algae, barnacles, mussels and oysters. Total coverage of organisms was analysed with ImageJ software (https://ij.imjoy.io/), during which



each image was converted to 8-bit grayscale, the darker areas isolated using a constant threshold, and the total darker area of each block calculated as percentage cover. This method isolated areas colonized by darker species, such as red algae, barnacles and oysters, but may provide a conservative estimate of cover since lighter shell areas and small barnacles may not have been detected.

2.6 Data analysis

Erosion of each sample over time during flume and field tests was calculated as loss rate (ε ; g g⁻¹ h⁻¹ or cm³ cm⁻³ h⁻¹). To calculate the loss rate, first the remaining fraction (ρ) of each sample was calculated (Equation 6):

$$\rho = \rho_0 / \rho_t \,. \tag{6}$$

For Xiriton bricks, this was calculated using the remaining height of the brick relative to the start point; for the smaller cylindrical samples, remaining fraction was calculated using the remaining sample volume or weight. To better account for potential measurement errors, the maximum likelihood estimation approach developed by Schotanus et al. (2020) was modified to assume that observations are independent over time. Consequently, the loss rate of each sample was estimated from remaining height or fraction, sampled at multiple time points, using Equation 7:

$$\varepsilon = (\frac{1}{n-1}) \sum_{i=1}^{n-1} 1 - \rho_{i+1}^{\frac{1}{l_{i+1}}}$$
 (7)

where n = number of measurements. In cases where ρ_{t_end} was equal or larger than ρ_0 , the loss rate was set to 0.

To investigate the effect of hydrodynamic activity on the erosion of Xiriton blocks, bed shear stress (τ) around the blocks was calculated both for the flume blocks and the field blocks. These estimations of the bed shear stress were used to relate the erosion rates in the flume with the field erosion. Flow velocity and bed roughness could not be obtained directly due to the flume set-up

and ADCP malfunctioning in the field, so the bed shear stress was estimated using calculated flow velocities and bed roughness parameters. The estimates of the bed shear stress are used for this purpose but cannot be taken as exact values.

To estimate the bed shear stress in the flume (τ_f , N m⁻²), the method of Marin-Diaz et al. (2022) was used. The bed shear stress in the flume was calculated using Equation 8:

$$\tau_f = \rho g(u^2/C^2) \tag{8}$$

where ρ = the density of salt water (kg m⁻³), u = water velocity in the flume (m s⁻¹)and C = Chézy coefficient (m^{0.5} s⁻¹). In the flume, the Chézy coefficient was approximated using Equation 9:

$$C = 18\log_{10}(12h_2/k_s) \tag{9}$$

where k_s = bed roughness in the flume (m), estimated as 0.0005 (Marin-Diaz et al., 2022).

For the data from the field, the bed shear stress was calculated for both the current (τ_c ; N m⁻²) and wave induced (τ_w ; N m⁻²) bed shear stress. τ_c was calculated using the same method as for τ_f . Here, the velocity used for the calculation was obtained using the maximum depth measured by the wave logger and the correlation of the maximum inundation depth and tidal induced current velocity obtained by Bouma et al. (2005). The Chézy coefficient was calculated using the maximum water depth for h_2 and a k_s of 0.001m (Equation 9).

 $\tau_{\rm w}$ was calculated using the water depth (h; m), wave height (H; m), wave period (T; s), measured with the pressure sensors, and the roughness height (r; m). Using linear wave theory and the method of Rijn (1993), $\tau_{\rm w}$ could then be calculated using Equation 10:

$$\tau_w = 1/4\rho_w f_w U_\delta^2 \tag{10}$$

where f_w = friction factor (-) and U_δ = peak bottom orbital velocity (m s⁻¹), which could both be derived from the measured data.

All statistical analyses of the results were performed using MATLAB (version 2021a) Statistics and Machine Learning

toolbox functions. N-way ANOVA tests and Tukey's Honest Significant difference (HSD) test were performed in stage 1 to compare loss rates between Xiriton XS5S-N4 and other concrete alternative materials (Table 1). ANOVA and Tukey's HSD tests were also used in stage 2 to compare compressive strength, erodibility (loss rates) and pH change between different Xiriton mixtures and between treatments, including the position of the block in the flume, curing period and water velocity to which the blocks were exposed. A Pearson correlation analysis was used to investigate the correlation between loss rates and bed shear stress in the fast flow flume (stage 2). Establishment of marine organisms onto three Xiriton blocks was compared using total percentage cover estimates, but statistical tests were not performed since these were preliminary tests without contrasting treatments.

3 Results

3.1 Production of Xiriton material

Xiriton was successfully produced in 5 different compositions, each with different characteristics (Table 2). The mixtures were possible to shape into both brick and cylindrical blocks (see Figures 2, 4) and appeared feasible to be moulded into a range of

shapes for different applications. All mixtures dried sufficiently to be removed from their moulds within the target drying period (3–8 weeks) and *Spartina anglica*, sourced from local saltmarshes, was effective as a binding fibre, since Xiriton mixtures remained intact during a range of flume and field exposure. The N5a mixture was the only material in any test to fully erode, due to its extremely low binder (pozzolan and lime) content; all other compositions of Xiriton, using both *Spartina anglica* and *Miscanthus giganteus*, had some material remaining following flume or wave exposure, as outlined below.

3.2 Xiriton compared to other building materials (stage 1 - testing)

When exposed to flow velocities of approximately 4.5 m s⁻¹ in a fast flow flume, neither Xiriton nor any of the comparison materials (non-Portland, non-Portland: strengthened and non-Portland: coconut fibre) eroded more than 2.5mm at any given point. Xiriton had a higher loss rate than each of the other materials (ANOVA, $F_{(3,236)} = 17.05$, p< 0.0001) (Figure 5A) indicating a slightly higher erodibility, although the average loss rate of Xiriton remained low, at 0.0031 \pm 0.0049 g g⁻¹ h⁻¹, indicating that total erosion was very little.

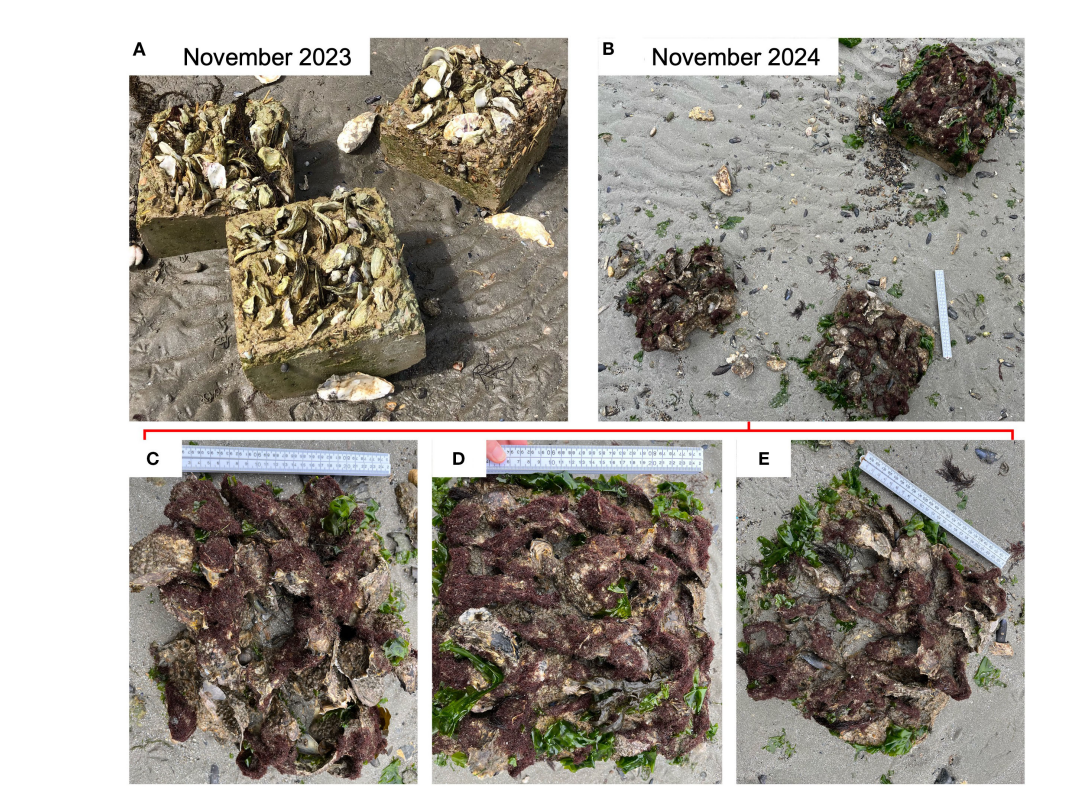


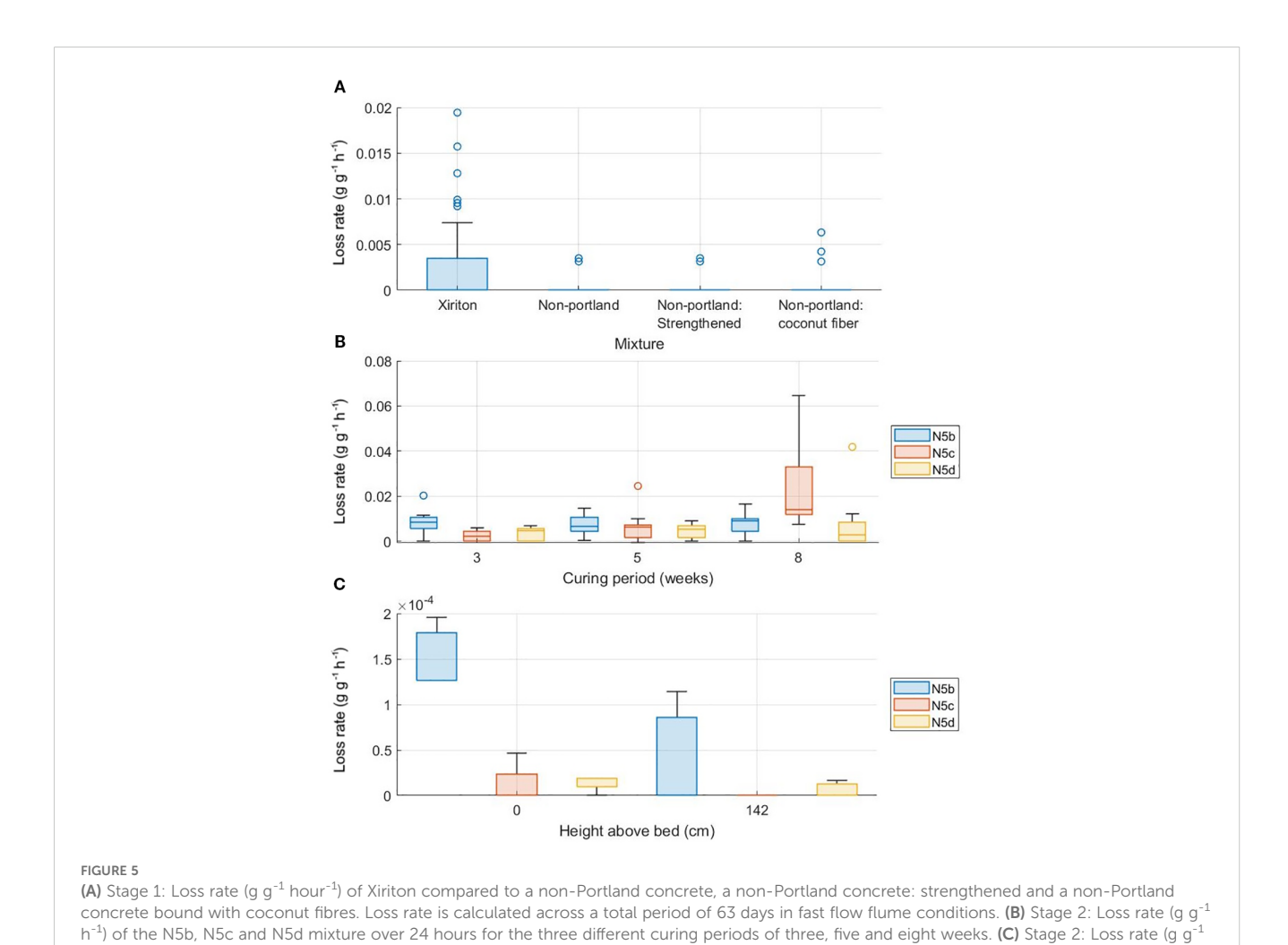
FIGURE 4
Three Xiriton blocks placed onto an intertidal flat in the Eastern Scheldt in November 2023. Blocks were initially placed dried, with oyster shells protruding from the mixture (A). (B–E) show the blocks 12 months later, in November 2024. Photos taken by Jim van Belzen and Victoria Mason.

3.3 Comparison of varying Xiriton mixtures (stage 2 - testing)

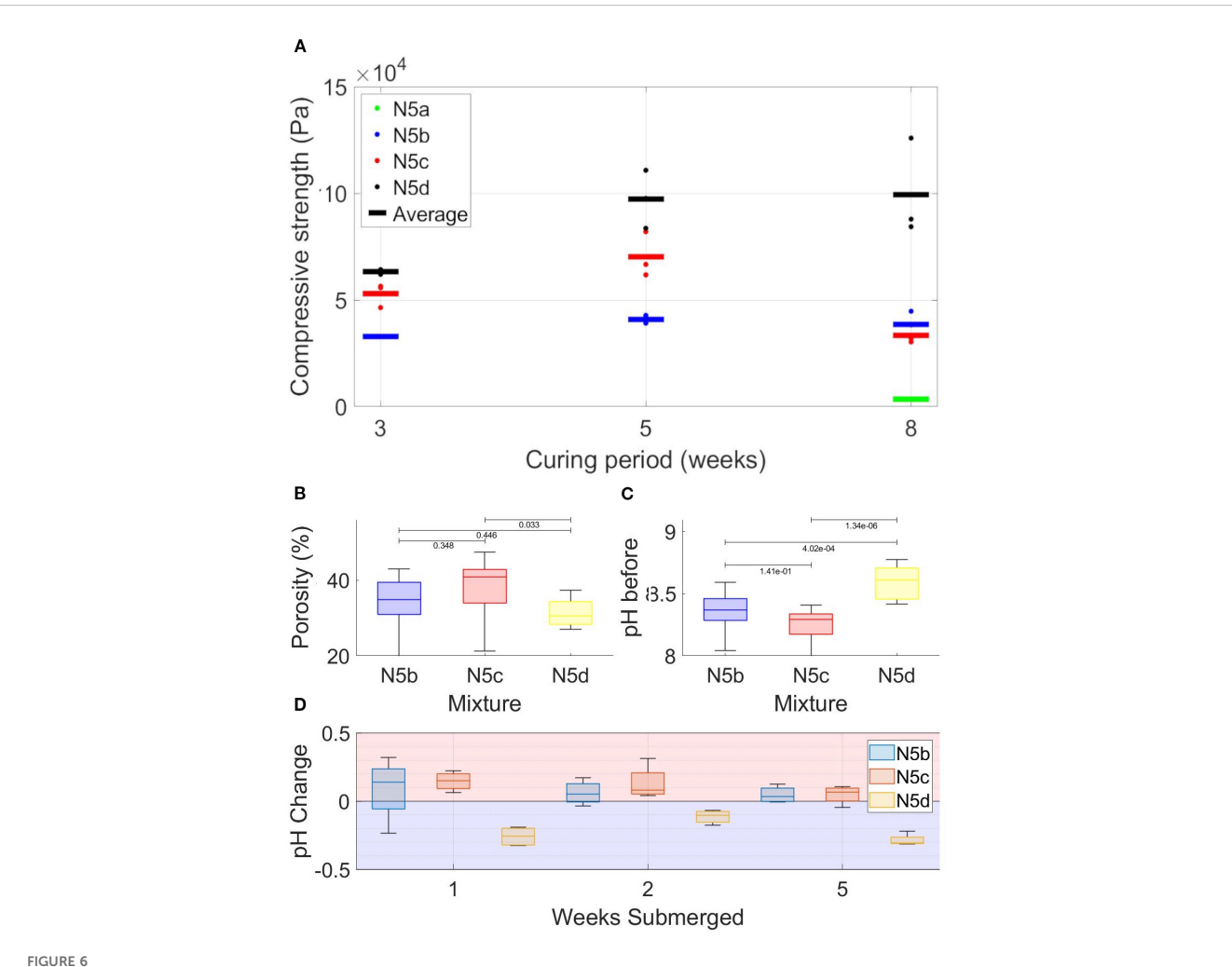
3.3.1 Experimental measurements: compressive strength, porosity and pH

Compressive strength of the Xiriton blocks increased with increasing quantities of binding material (pozzolan and slaked lime) and shell material (Figure 6A). The mixture with the least binding materials, N5a, was substantially weaker than the other three mixtures, to a greater extent even than shown in the data. Since some N5a measurements recorded no breaking point, this indicates that those mixtures crumbled easily. In mixtures N5c and N5d, curing time had an influence on compressive strength (ANOVA, $F_{(2.6)} = 18.9$, p = 0.0026 for N5c and ANOVA, $F_{(2.6)} =$ 5.18, p = 0.049 for N5d). A follow up Tukey test showed that for the N5c mixture, the compressive strength was lower after an 8-week curing period compared to a 3 or 5-week curing period (p = 0.041 and p = 0.0021 respectively, df (degrees of freedom) = 8); although a similar pattern was observed for N5a and N5b, these results were not significant. In the N5d mixture, compressive strength was highest after an 8-week curing period, and lowest after 3 weeks, although the Tukey test did not indicate significant differences (p = 0.065, df = 8). There were therefore circumstances in which a longer curing period either strengthened or weakened the block, depending on the mixture.

The N5a mixture was excluded from porosity and pH testing since all blocks had eroded very quickly. Porosity was significantly different between mixtures (ANOVA, $F_{(2,33)} = 3.48$, p = 0.042) and the follow up Tukey test showed a significant lower porosity for N5d compared to N5c (p = 0.033, df = 33), but no significant differences with N5b [p = 0.35 and p = 0.45, df = 33, for n5c and N5d,respectively (Figure 6B)]. All three mixtures had a slightly alkaline pH (7.99 - 8.78), with N5c the least alkaline mixture and N5d the most alkaline mixture (Figure 6C). pH changes after submergence were relatively small (-0.33 - 0.32). Mixtures N5b and N5c became slightly more alkaline after submergence in seawater, while N5d, the most alkaline mixture at the start, became slightly less alkaline and shifted closer to a neutral pH, and to the pH of the other mixtures, after all submergence times (Figure 6D). After submergence, there remained a significant difference between the mixtures (ANOVA, F (2.33) = 5.10, p = 0.012), with the follow up Tukey test showing that this was the case for N5b and N5c (p = 0.012, df = 33, Figure 6D).



h⁻¹) for the N5b, N5c and N5d mixtures placed on the intertidal flat for 63 days (height above bed = 0m) and 70 days (height above bed = 142m)



Compressive strength, porosity and pH characteristics of the N5b, N5c and N5d Xiriton mixtures (N5a values only obtained for the compressive strength due to immediate erosion under testing). (A) shows the compressive strength (Pa \leftrightarrow N m⁻²) after 3, 5 and 8 weeks of curing for the four Xiriton mixtures. (B) shows porosity (%) of each mixture, (C) shows pH of each mixture and (D) shows pH change after 1, 2 and 5 weeks submerged in seawater. A negative value (red) indicates a shift towards a less alkaline (more acidic) pH, a positive value (blue) indicates a shift towards a more alkaline pH.

3.3.2 Erodibility of varying Xiriton mixtures in flume conditions

Under a super critical flow regime in the fast flow flume, the N5a eroded rapidly (100% erosion over 24 hours), and very little erosion occurred for N5b, N5c and N5d (0-5% over 24 hours) (Figure 5B). Most erosion was observed in the first 5 hours of testing, with the N5a mixture usually completely eroded within 1 hour. ANOVA testing showed that the position of the blocks (in the flume (ANOVA, $F_{(2,189)} = 2.71$, p = 0.0695), slot (ANOVA, $F_{(3,188)} = 0.18$, p = 0.907) and location in the slot (ANOVA, $F_{(3,188)} = 0.21$, p = 0.8925) did not influence the erosion of the blocks. There was also no significant difference in erosion between different water velocities (ANOVA, $F_{(3,188)} = 2.43$, p = 0.0668), but the Pearson correlation test, conducted on each mixture separately, did show a significant positive correlation between flow velocity and erosion for all mixtures (Table 3).

Erosion of the blocks under different flow velocities depended on the mixture type (ANOVA, $F_{(3,188)} = 873.11$, p< 0.001). The

difference between erosion was largely driven by the rapid erosion of the N5a mixture, which eroded significantly more than each of the 3 other mixtures (Tukey test, p< 0.001, d = 177 in all cases). Due to the strong influence of the N5a erosion on the test result, a further ANOVA was performed which excluded the N5a mixture. In this test none of the factors showed a significant influence on the erosion. A following Tukey test (due to a near-significant ANOVA ($F_{(2,141)}=2.93,\ p=0.0568$)) showed a decrease in mean loss rate from N5b to N5d, with a significantly higher mean loss rate for N5b compared to N5d ($p=0.043,\ df=130$). Mean loss rate for N5c was between the two other mixtures, but not significantly different to either ($p=0.6113,\ df=130$ compared to N5b and $p=0.3116,\ df=130$ compared to N5d).

The results of erodibility with varying curing periods excluding N5a showed that both curing period (ANOVA, $F_{(2,105)} = 7.87$ and p< 0.001) and mixture type (ANOVA, $F_{(2,105)} = 3.44$ and p = 0.0361) significantly influenced erosion. There were small differences in the erosion of N5b, N5c and N5d, with N5b

TABLE 3 The average water velocity (m s ⁻¹), bed shear stress (N m ⁻²) and loss rate (g g ⁻¹ h ⁻¹) for every velocity experiment (Vel 1,2,3, and 4) with the
Pearson correlation for the relation between the loss rate and bed shear stress for each mixture.

		Vel 1	Vel 2	Vel 3	Vel 4	Pearson cor	relation
Average water velocity (m s ⁻¹)		1.69	2.33	3.03	4.20		
Average bed shear stress (N m ⁻²)		12.9	29.26	61.56	122.6	R	p
Loss rate (ε, g g ⁻¹ h ⁻¹)	N5a	0.6997	0.9395	0.9418	0.9439	0.31	0.033
	N5b	0.0057	0.0044	0.0068	0.0087	0.34	0.019
	N5c	0.0033	0.0047	0.0063	0.0081	0.32	0.027
	N5d	0.0030	0.0040	0.0046	0.0060	0.41	0.0039

eroding the most, except after an 8-week curing period (Figure 5B). This reflected the physical properties of the mixtures, where there was an increase in compressive strength from N5a to N5d. The effect of the curing period was driven by large differences in erosion of the N5c mixture after an 8-week curing period (ANOVA, $F_{(2,33)} = 11.12$, p<0.001), where loss rate significantly increased (p<0.001, Figure 5B). The increase in loss rate for N5c from 3 and 5 weeks to 8 weeks was over 10 times greater than for N5b and N5d.

3.3.3 Erodibility of varying Xiriton mixtures in intertidal conditions

Erosion of the Xiriton blocks on the intertidal flat followed similar patterns to erosion in the flume (Figure 5C). The N5a mixtures had completely eroded before the first measurement, after 3 days. Since volume displacement measurements were used for loss rate calculation and only taken at the end of the field experiment when N5a had eroded, N5a blocks were excluded from statistical analysis. Mixture type significantly influenced erosion of the 3 remaining mixtures (ANOVA, $F_{(2,17)} = 6.91$, p = 0.0114). Height above the bed and position on the frame did not significantly affect loss rate. The follow up Tukey test showed that N5b eroded significantly more than N5c and N5d (p = 0.0199, df = 11 and p = 0.0176, df = 11, respectively), but there was no significant difference between the erosion of mixtures N5c and N5d (p = 0.995, df = 11). Maximum bed shear stress was at least 50x lower than in the flume (0.23 N m⁻² for the current induced bed shear stress and 0.055 N m⁻² for the wave induced bed shear stress), nevertheless significant erosion was visible in the field (Figure 5C).

3.4 Establishment of marine organisms (stage 3 - testing)

Following a 12-month deployment on an intertidal mudflat, each of the three Xiriton blocks remained present, although all blocks had experienced erosion on the surface and sides. Species of green algae (*Ulva lactuca*) and brown algae (*Fucus vesiculosus*) had attached to all three of the blocks, as well as widespread barnacles (predominantly *Balanus crenatus*, with some *Balanus balanoides*)

and periwinkles (predominantly *Littorina littorea*). Blue mussels (*Mytilus edulis*) and Pacific oysters (*Crassostrea gigas*) were often found between protruding oyster shells from the original mixture. Total percentage cover was relatively consistent between each block with 71.4% cover on block A, 70.4% cover on block B and 69.3% cover on block C. While these cover estimates only provide an approximate estimate of total organism cover on the top of the structures (not including the sides), they indicate that colonization of the blocks within a year was relatively high and did not depend on the position of the blocks relative to each other.

4 Discussion and conclusions

4.1 Overall findings on the performance of Xiriton for application in nature

Early investigation indicates that Xiriton, a novel and sustainable concrete alternative, has potential as a material for use in NbS. Xiriton could provide additional building options in scenarios where limitations of conventional building materials may hinder their use, such as expensive production (e.g. biodegradable plastic alternatives (Nitsch et al., 2021) for largescale applications, damaging environmental impacts of concrete and rocks (Hillier et al., 1999; Setunge et al., 2009) in vulnerable ecosystems and lack of flexibility in shaping, and unknown/ uncontrollable lifetime where structures are only required for a short time period. We show via laboratory, flume and field testing that Xiriton may overcome many such limitations and become a valuable addition to the current repertoire of available materials for coastal structures, particularly where non-permanent structures are required. For example, varying the content of binding material (pozzolan and slaked lime) in the mixture resulted in differing erosion rates in both fast flow flume and field settings. Specifically, mixture N5a, with minimal binding material, eroded much faster than any of the mixtures with a greater quantity of binding material. In addition, the baseline (XS5S-N4, including Spartina anglica vegetation) Xiriton mixture showed comparable erosion to other alternative building materials. pH testing showed a value of around

8–9, indicating weak alkalinity. This is considerably lower than the pH of conventional concrete, which can reach around 13 (Behnood et al., 2016; Li et al., 2021). Additionally, we only observed minimal changes in pH over time. This, combined with the demonstrated possibility to use locally sourced (e.g. saltmarsh based) ingredients, strongly reduces the environmental impact of Xiriton both during its lifetime and following degradation. Early settlement tests in a mesotidal system demonstrate that Xiriton may allow rapid establishment of marine organisms such as algae and bivalves, which could potentially boost biodiversity. In short, while longer-term studies remain needed to fully understand the scope, limitations and impacts of the application of Xiriton, early results indicate that Xiriton may in some cases provide a more ecologically beneficial alternative to conventional building materials without sacrificing reliability.

4.2 Potential of Xiriton as a material with adjustable erodibility

The ability to adjust the degradability of a material becomes particularly relevant when it is considered for use in coastal ecosystems, since this makes it applicable for a range of purposes in an often highly dynamic environment. For example, Xiriton could be used to boost the establishment of shellfish reefs, in which case a relatively short lifespan of 1–5 years would allow oyster larvae to settle and establish into a reef (Ridge et al., 2015). The use of locally-sourced raw materials prevents the need to remove the structures in the years after reef initiation, which could otherwise be very damaging to the newly established reef (Nordstrom, 2014). Eco-engineering materials have also been deployed in front of saltmarsh edges to reduce lateral erosion and subsequent marsh narrowing (Van Loon-Steensma and Slim, 2013; Marin-Diaz et al., 2021). In this case, elevations may be too high in a meso- or macrotidal system to allow oyster establishment (Fivash et al., 2021) and therefore the structure itself will be required to remain in-situ for longer to attenuate waves and encourage sediment deposition. In such a scenario, the ability to adjust the erodibility of Xiriton would be useful; where cycles of marsh expansion and retreat are typically in the order of decades (Bouma et al., 2016), applying a material with a comparable timespan may be most appropriate to reduce the need for further intervention. Similarly, the adjustable erodibility of Xiriton may be useful in creating biodegradable weights for biodegradable subtidal reef-restorations structures, such as, for example, TreeReefs (Dickson et al., 2023). Xiriton's potential applications likely extend beyond those discussed above. When its erodibility is adjusted, by tuning the ratios of raw materials, it can be designed to break down into non-harmful, locally sourced components within the project's expected lifespan and permit period. In such cases, removing Xiriton structures should not be necessary, which reduces the costs of returning to a site for material removal. This flexibility in erodibility could not only expand Xiriton's range of uses but also lower the long-term management costs of coastal ecosystems.

Regardless of the mixture and the subsequent lifetime of Xiriton, it is likely that all the material will eventually erode, given the dynamic nature of intertidal environments (Le Hir et al., 2000). A critical feature of Xiriton is therefore the ability to construct it from locallysourced ingredients, such as saltmarsh vegetation (here Spartina anglica), crushed oyster shells, and sand. Whether a structure degrades in one month or over twenty years, limiting the materials left behind to those found naturally in the environment will inherently minimise its long-term impacts. In order to upscale the production of Xiriton with these properties in different locations globally, vegetation with similar properties, for example, bamboo or giant reed (Arundo donax), and the potential for sustainable harvesting, will need to be identified. Conventional concretes have been found, in some cases, to leach heavy metals into the environment (Hillier et al., 1999) and many bioplastics or plastic alternatives still have unknown or toxic breakdown products (Zimmermann et al., 2020). The result that Xiriton erodibility can be easily adjusted within the constraints of largely locally sourced ingredients therefore represents a promising step forward in the development of construction materials with minimal long-term persistence in the marine environment. It should, however, be noted that such erodibility makes Xiriton applicable in cases where shorter-term persistence is desirable but may make it unsuitable in cases where permanent structures are required, unless used as a 'hybrid' solution with other, longerlasting materials.

4.3 Ecological benefits, potential uses and limitations of Xiriton

A limitation of the use of conventional concrete in coastal settings is the likelihood of pH changes to the nearby environment; when submerged, concrete may leach Ca(OH)2 and thus alter the carbon chemistry of the directly surrounding water (Anderson and Underwood, 1994). These chemical and subsequent pH changes (alkalisation) are likely to influence which organisms establish on the structures and potentially the surrounding area (Glasby, 2000). While it has been suggested that the alkalisation effect of concrete may have a positive influence on establishment of marine organisms, since it can act as a local buffer to ocean acidification (Mos et al., 2019), it is often observed that colonisation is delayed. Xiriton had a slightly alkaline surface pH, but similarly to newer materials such as ECOncrete (Ido and Shimrit, 2015), showed very small pH changes when submerged in seawater. The slightly alkaline surface pH may offer a similar buffering effect for settling organisms (Mos et al., 2019), but maximum pH change over time was in the order of 0.2, indicating that large leaching effects in the surrounding seawater are unlikely. Our measurements of pH change were taken over a relatively short period, so longer term assessment of the chemical impact of Xiriton when submerged, and when repeatedly submerged-exposed, is necessary.

Settlement of a range of organisms onto Xiriton blocks over a 12-month period in a mesotidal system suggest that it may be used to stimulate organism settlement across a variety of contexts, a

proxy indicating that Xiriton may be used to enhance biodiversity. While Miscanthus giganteus was used in the blocks tested for settlement, similar patterns are likely to be observed with similarly structured C4 grass species such as Spartina anglica. Organisms established on the Xiriton blocks spanned a range of functional groups, including green algae, brown algae and bivalves. The presence of juvenile blue mussels (Mytilus edulis) and Pacific oysters (Crassostrea gigas) in particular indicates the potential for Xiriton to be used to initiate the formation of shellfish reefs. It is likely that establishment onto Xiriton blocks could be further enhanced by using bio-mimicry designs (Temmink et al., 2023) and consequently experimenting with different shapes and surface complexities, since both have been found to influence niches available for establishing organisms (Loke et al., 2015, 2017; Strain et al., 2018; Riera et al., 2024) and fish communities (Hackradt et al., 2011). Similarly, creating blocks with fresh oyster shells compared to older shells may enhance chemical cues, which encourage the settlement of oyster larvae (Tamburri et al., 2008). As frequently observed with standard concrete structures, different mixtures (Natanzi et al., 2021) and orientations (Becker et al., 2020) of Xiriton are also likely to lead to different communities of settling organisms. Nonetheless, the presence of around 70% cover of sessile organisms on every Xiriton block remaining in the field suggests that the material overall offers a suitable substrate for establishment.

While the potential applications for Xiriton are clear and wide ranging, there will be scenarios in which it is not the most suitable material and conventional materials will be used. For example, where more permanent structures are needed for coastal defence, longer lasting materials such as rocks may be more applicable, or where construction time is limited, brushwood dams may be a faster solution. The rapid progress in the field of bioplastics is also greatly increasing the flexibility and reducing the impact of such materials, which may support their use in scenarios where more intricate structures are required than those possible from Xiriton. We also highlight the necessity to consider the system on a larger-scale when making the decision on whether to implement any type of manmade structures. For example, while Xiriton structures may help to protect saltmarsh edges from erosion by attenuating waves and encouraging sediment deposition, such erosion may be the result of estuary or coastline scale changes which influence sediment supply and hydrodynamics (e.g. dredging activities and channel migration) (Van der Wal et al., 2008). The expansion and retreat of vegetated ecosystems is also a frequently seen cycle (van de Koppel et al., 2005; Van der Wal et al., 2008; Bouma et al., 2016); placing structures to influence these cycles may therefore be highly useful when maintaining ecosystem area for ecosystem service provision or where climate-change induced erosion becomes persistent, but unnecessary in other scenarios where there is space to allow for natural marsh-dynamics and coupled species rejuvenation. An indepth and integrated assessment of ecosystem dynamics within the broader landscape context is essential as a foundational step before introducing materials like Xiriton into natural systems.

4.4 Challenges and future research directions

In this study, we aimed to provide an initial indication of the applicability of Xiriton for use in intertidal systems, which gave a positive view of its potential. Further testing to overcome timerestricted measurement limitations is essential to provide a more comprehensive overview of the properties and behaviour of the material on longer time scales. For example, our erosion experiments primarily focussed on water erosion as the determining factor in the weathering of Xiriton structures, which is likely the case (Ma et al., 2023). However, the exact influence of other factors, such as climate, UV exposure and drying/rewetting cycles, is still unstudied. For example, climate conditions that can expose structures to freezing/thawing cycles may reduce the compressive strength of Xiriton, a process known to occur in conventional concrete (Peng et al., 2022). Similarly, in areas with high light exposure, which may be amplified by longer emersion times, exposure to ultraviolet (UV) radiation has the potential to influence the structural integrity of the material, given that this has been observed in cement-based compounds (Wang et al., 2022). The position at which a structure is placed in the tidal frame will influence also its exposure time and drying/rewetting cycles (Zhang et al., 2021). In our study, field tests on Xiriton were conducted in a mesotidal system. However, in a microtidal or macrotidal system, with smaller or larger variations in emergence time, respectively, drying/rewetting cycles will differ from those observed here and thus should be tested before upscaling. During the production stage, curing under different temperatures may affect the porosity of C-S-H compounds (Bahafid et al., 2017) present in Xiriton, while differing compositions of sand, seawater and binding agents could have minor influences on the structure of Xiriton produced in different locations. Such processes may in turn affect the erosion rate of the structure, which could result in a different lifetime of the material in changing climate conditions and inundation regimes. As such, the mixtures used in this study aim to present a template for the production and upscaling of Xiriton in other locations worldwide, rather than a definitive indication of structural properties under any condition.

As the aimed lifetime of Xiriton can range from months to decades, it is beneficial to use enhanced weathering simulations such as those used in this research to obtain results in shorter time frames. However, weathering under these techniques may not always be directly translated from a controlled simulation to actual field conditions. Here, an approximation of the bed shear stress was used to relate flume results with field conditions. However, erosion and bed shear stress are not linearly correlated (Keshavarz et al., 2024). For erosion to occur, a critical bed shear stress typically must be reached (San Juan et al., 2024). Depending on the material, erosion may not occur linearly by scraping off the edges of the structure, or more as a chunk-by-chunk process. Similar stochastic erosion events were observed in studies that investigated the erosion of consolidated clay (Lick and McNeil,

2001; Das et al., 2019; San Juan et al., 2024). Such a change in the erosion process between mixtures could be an explanation for the increased erosion of Xiriton-N5c after a longer curing period and should be explored as an additional mechanism for Xiriton erosion.

There are almost unlimited possible mixtures of Xiriton that could be produced, using widely available materials found worldwide (such as C4 grasses, pozzolan, sand and crushed shells). The availability of these Xiriton ingredients contributes to their relatively low cost in many locations worldwide, which may be amplified by the use of, for example, biproducts from local shellfish aquaculture for the shell component of the mixture. Combining locally adaptable recipes with simple mixing procedures, flexible mould construction (e.g. simple wooden boxes) and the ability to deploy by boat or on foot (where applicable) allows the potential for global upscaling of Xiriton deployment. In this paper, we showed the effect of different ratios in the mixture on the erosion rate of the blocks. However, there is an opportunity to further vary ingredients to influence erodibility and settlement or to ensure that vegetation included is local to the deployment site. Since different stem lengths could change the cohesion of the block structure (Ahmad et al., 2020), the development of a portfolio of design options and recipes of possible Xiriton structures could be a useful step towards adapting Xiriton production to a range of applications, particularly where it may be used on a larger scale (Supplementary Table S1). Within this portfolio, standardised compressive strength measurements of the different recipes could be used as a comparison tool of the recipes, so that an estimation of the lifetime can be made before use of the recipe. In addition to such a portfolio, a full life-cycle assessment, including costbenefit analysis, of different Xiriton mixtures and other comparable concrete alternatives will be a critical next step in the application of structures with adjustable erodibility into coastal management strategies.

4.5 Conclusions

Initial testing of Xiriton indicates adjustable erodibility and lifetime, minimal environmental impacts in terms of pH and waste products, and the potential to easily shape towards different purposes to enable upscaling in a cost effective and locally adaptable way. Xiriton may provide an avenue by which to build structures which conserve natural systems, while leaving minimal traces of intervention into the future. In short, building with Xiriton from locally sourced raw materials is an example of an approach with the objective of contributing towards the establishment of self-sustaining systems, rather than remaining longer-term. The potential for using Xiriton within NbS is evident; the application of Xiriton in intertidal systems now depends principally on further research into long-term impacts and strategies by which to upscale the building and deployment processes.

Data availability statement

The data from this study (article and Supplementary Material) are openly available in the research repository 4TU: https://data.4tu.nl/datasets/7ead96aa-d52c-4cfd-9074-1aebc27143e6. Further inquiries can be directed to the corresponding authors.

Author contributions

VM: Resources, Writing – review & editing, Formal analysis, Visualization, Methodology, Writing – original draft, Conceptualization, Investigation. JeV: Methodology, Writing – original draft, Conceptualization, Investigation, Visualization, Writing – review & editing, Resources, Formal analysis. TB: Writing – review & editing, Methodology, Supervision, Funding acquisition, Conceptualization. DS: Writing – review & editing, Investigation, Methodology. DV: Methodology, Writing – review & editing, Investigation. TV: Resources, Writing – review & editing, Supervision, Conceptualization. RT: Methodology, Resources, Conceptualization, Writing – review & editing. FB: Methodology, Investigation, Conceptualization, Resources, Writing – review & editing. JiV: Conceptualization, Writing – review & editing, Investigation, Supervision.

Funding

The author(s) declare that no financial support was received for the research, and/or publication of this article.

Acknowledgments

We would like to thank The Fieldwork Company, particularly Tom van Leusden, for their help producing flume samples and Lennart van IJzerloo and Daniel Blok for their extremely helpful technical support. We also thank Charlotte Bruggeman and Hugo Thijssens for their internship work which contributed to the Xiriton testing, and Alex Ji and other NIOZ interns that kindly assisted with flume measurements. We are grateful for permission from Natuurmonumenten to perform the measurements at Rattekaai, NL. The input from Victoria Mason and Tjeerd Bouma was supported by the 'LIVING DIKES - Realising Resilient and Climate-Proof Coastal Protection' project (with project number NWA.1292.19.257) of the NWA research program 'Research on Routes by Consortia (ORC)', which is funded by the Netherlands Organization for Scientific Research (NWO). Daniel Varley, Tjisse van der Heide and Ralph J.M. Temmink were supported by Waddenfonds grant 'Bouwen met Biobouwers'.

Conflict of interest

The authors declare that the research was conducted in the absence of any commercial or financial relationships that could be construed as a potential conflict of interest.

Generative AI statement

The author(s) declare that no Generative AI was used in the creation of this manuscript.

Any alternative text (alt text) provided alongside figures in this article has been generated by Frontiers with the support of artificial intelligence and reasonable efforts have been made to ensure accuracy, including review by the authors wherever possible. If you identify any issues, please contact us.

Publisher's note

All claims expressed in this article are solely those of the authors and do not necessarily represent those of their affiliated organizations, or those of the publisher, the editors and the reviewers. Any product that may be evaluated in this article, or claim that may be made by its manufacturer, is not guaranteed or endorsed by the publisher.

Supplementary material

The Supplementary Material for this article can be found online at: https://www.frontiersin.org/articles/10.3389/fmars.2025.1661288/full#supplementary-material

References

Achternbosch, M., Kupsch, C., Nieke, E., and Sardemann, G. (2011). Climate-friendly production of cement: A utopian vision? *GAIA - Ecol. Perspect. Sci Soc.* 20, 31–40. doi: 10.14512/GAIA.20.1.8

Ahmad, W., Farooq, S. H., Usman, M., Khan, M., Ahmad, A., Aslam, F., et al. (2020). Effect of coconut fiber length and content on properties of high strength concrete. *Materials* 13, 1075. doi: 10.3390/MA13051075

Anderson, M. J., and Underwood, A. J. (1994). Effects of substratum on the recruitment and development of an intertidal estuarine fouling assemblage. *J. Exp. Mar. Biol. Ecol.* doi: 10.1016/0022-0981(94)90006-X

Ashis, M. (2015). Application of geotextiles in Coastal Protection and Coastal Engineering Works: An overview. *Int. Res. J. Environ. Sci. Int. Sci Congress Assoc.* 4, 96–103.

ASTM International Subcomittee C09.61 (2014). Test method for compressive strength of cylindrical concrete specimens (ASTM C39/C39M-14) (West Conshohocken, PA). doi: 10.1520/C0039_C0039M-14

Bahafid, S., Ghabezloo, S., Duc, M., Faure, P., and Sulem, J. (2017). Effect of the hydration temperature on the microstructure of Class G cement: C-S-H composition and density. *Cement Concrete Res.* 95, 270–281. doi: 10.1016/J.CEMCONRES.2017.02.008

Balke, T., Bouma, T. J., Horstman, E. M., Webb, E. L., Erftemeijer, P. L. A., and Herman, P. M. J. (2011). Windows of opportunity: Thresholds to mangrove seedling establishment on tidal flats. *Mar. Ecol. Prog. Ser.* 440, 1–9. doi: 10.3354/MEPS09364

Balke, T., Herman, P. M. J., and Bouma, T. J. (2014). Critical transitions in disturbance-driven ecosystems: identifying Windows of Opportunity for recovery. *J. Ecol.* 102, 700–708, doi: 10.1111/1365-2745.12241

Barausse, A., Grechi, L., Martinello, N., Musner, T., Smania, D., Zangaglia, A., et al. (2015). An integrated approach to prevent the erosion of salt marshes in the lagoon of Venice. *EQA - Int. J. Environ. Qual.* 18, 43–54. doi: 10.6092/ISSN.2281-4485/5799

Becker, L. R., Ehrenberg, A., Feldrappe, V., Kröncke, I., and Bischof, K. (2020). The role of artificial material for benthic communities – Establishing different concrete materials as hard bottom environments. *Mar. Environ. Res.* 161, 105081. doi: 10.1016/j.marenvres.2020.105081

Behnood, A., Van Tittelboom, K., and De Belie, N. (2016). Methods for measuring pH in concrete: A review. *Construction Building Materials* 105, 176–188. doi: 10.1016/J.CONBUILDMAT.2015.12.032

Bersoza Hernández, A., Brumbaugh, R. D., Frederick, P., Grizzle, R., Luckenbach, M. W., Peterson, C. H., et al (2018). Restoring the eastern oyster: how much progress has been made in 53 years? *Front. Ecol. Environ.* 16 (8), 463–471. doi: 10.1002/FEE.1935

Borsje, B. W., van Wesenbeeck, B. K., Dekker, F., Paalvast, P., Bouma, T. J., van Katwijk, M. M., et al. (2011). How ecological engineering can serve in coastal protection. *Ecol. Eng.* 37, 113–122. doi: 10.1016/j.ecoleng.2010.11.027

Bouma, T. J., de Vries, M. B., Low, E., Kusters, L., Herman, P. M. J., Tánczos, I. C., et al. (2005). Flow hydrodynamics on a mudflat and in salt marsh vegetation: Identifying general relationships for habitat characterisations. *Hydrobiologia* 540, 259–274. doi: 10.1007/s10750-004-7149-0

Bouma, T. J., van Belzen, J., Balke, T., Zhu, Z., Airoldi, L., Blight, A. J., et al. (2014). Identifying knowledge gaps hampering application of intertidal habitats in coastal protection: Opportunities & steps to take. *Coast. Eng.* 87, 147–157. doi: 10.1016/j.coastaleng.2013.11.014

Bouma, T. J., van Belzen, J., Balke, T., van Dalen, J., Klaassen, P., Hartog, A. M., et al. (2016). Short-term mudflat dynamics drive long-term cyclic salt marsh dynamics. *Limnology Oceanography* 61, 2261–2275. doi: 10.1002/LNO.10374

Bucher, F. J. (2022). Xiriton. landscaped carbon capture and storage in architecture (lccsa).

Campbell, A. D., Fatoyinbo, L., Goldberg, L., and Lagomasino, D. (2022). Global hotspots of salt marsh change and carbon emissions. *Nature* 612, 701–706. doi: 10.1038/s41586-022-05355-z

Cao, H., Zhu, Z., James, R., Herman, P. M. J., Zhang, L., Yuan, L., et al. (2020). Wave effects on seedling establishment of three pioneer marsh species: survival, morphology and biomechanics. *Ann. Bot.* 125, 345–352. doi: 10.1093/AOB/MCZ136

Chowdhury, M. S. N., Walles, B., Sharifuzzaman, S., Shahadat Hossain, M., Ysebaert, T., and Smaal, A. C.. (2019).) Oyster breakwater reefs promote adjacent mudflat stability and salt marsh growth in a monsoon dominated subtropical coast. *Sci. Rep.* 9, 8549. doi: 10.1038/s41598-019-44925-6

Comba, D., Palmer, T. A., Breaux, N. J., and Pollack, J. B. (2023). Evaluating biodegradable alternatives to plastic mesh for small-scale oyster reef restoration. *Restor. Ecol.* 31, e13762. doi: 10.1111/REC.13762

Corbella, S., and Stretch, D. D. (2012). Geotextile sand filled containers as coastal defence: South African experience. *Geotextiles Geomembranes* 35, 120–130. doi: 10.1016/J.GEOTEXMEM.2012.09.004

Das, V. K., Roy, S., Barman, K., Chaudhuri, S., and Debnath, K. (2019). Study of claysand network structures and its effect on river bank erosion: an experimental approach. *Environ. Earth Sci.* 78, 591. doi: 10.1007/S12665-019-8613-5

Davis, J. L., Currin, C. A., O'Brien, C., Raffenburg, C., and Davis, A.. (2015). Living shorelines: coastal resilience with a blue carbon benefit. *PloS One* 10, e0142595. doi: 10.1371/JOURNAL.PONE.0142595

de Vet, P. L. M., van Prooijen, B. C., and Wang, Z. B. (2017). The differences in morphological development between the intertidal flats of the Eastern and Western Scheldt. *Geomorphology* 281, 31–42. doi: 10.1016/J.GEOMORPH.2016.12.031

Dickson, J., Franken, O., Watson, M. S., Monnich, B., Holthuijsen, S., Eriksson, B. K., et al. (2023). Who lives in a pear tree under the sea? A first look at tree reefs as a complex natural biodegradable structure to enhance biodiversity in marine systems. *Front. Mar. Sci* 10. doi: 10.3389/FMARS.2023.1213790/BIBTEX

Dunstan, E. R. (2011). How Does Pozzolanic Reaction Make Concrete "Green". Available online at: http://www.flyash.info/ (Accessed January 28, 2025).

Fivash, G. S., Stüben, D., Bachmann, M., Walles, B., van Belzen, J., Didderen, K., et al. (2021). Can we enhance ecosystem-based coastal defense by connecting oysters to marsh edges? Analyzing the limits of oyster reef establishment. *Ecol. Eng.* 165, 106221. doi: 10.1016/j.ecoleng.2021.106221

Gedan, K. B., Kirwan, M. L., Wolanski, E., Barbier, E. B., Silliman, B. R., Gedan, K. B., et al. (2011). The present and future role of coastal wetland vegetation in protecting shorelines: answering recent challenges to the paradigm. *Climatic Change* 106, 7–29. doi: 10.1007/s10584-010-0003-7

Ghahari, S. A., Mohammadi, A., and Ramezanianpour, A. A. (2017). Performance assessment of natural pozzolan roller compacted concrete pavements. *Case Stud. Construction Materials* 7, 82–90. doi: 10.1016/J.CSCM.2017.03.004

Glasby, T. M. (2000). Surface composition and orientation interact to affect subtidal epibiota. J. Exp. Mar. Biol. Ecol. 248, 177–190. doi: 10.1016/S0022-0981(00)00169-6

Green, D. S., Chapman, M. G., and Blockley, D. J. (2012). Ecological consequences of the type of rock used in the construction of artificial boulder-fields. *Ecol. Eng.* 46, 1–10. doi: 10.1016/J.ECOLENG.2012.04.030

Hackradt, C. W., Félix-Hackradt, F. C., and García-Charton, J. A. (2011). Influence of habitat structure on fish assemblage of an artificial reef in southern Brazil. *Mar. Environ. Res.* 72, 235–247. doi: 10.1016/j.marenvres.2011.09.006

Hillier, S. R., Sangha, C. M., Plunkett, B. A., and Walden, P. J.. (1999). Long-term leaching of toxic trace metals from Portland cement concrete. *Cement Concrete Res.* 29, 515–521. doi: 10.1016/S0008-8846(98)00200-2

Hinkel, J., Lincke, D., Vafeidis, A. T., Perrette, M., Nicholls, R. J., Tol, R. S. J., et al. (2014). Coastal flood damage and adaptation costs under 21st century sea-level rise. *Proc. Natl. Acad. Sci. United States America* 111, 3292–3297. doi: 10.1073/pnas.1222469111

Howie, A. H., and Bishop, M. J. (2021). Contemporary oyster reef restoration: responding to a changing world. *Front. Ecol. Evol.* 9. doi: 10.3389/FEVO.2021.689915/BIBTEX

Ido, S., and Shimrit, P. F. (2015). Blue is the new green – Ecological enhancement of concrete based coastal and marine infrastructure. *Ecol. Eng.* 84, 260–272. doi: 10.1016/ I.ECOLENG.2015.09.016

Indrawati, V., and Manaf, A. (2008). Mechanical strength of trass as supplementary cementing material. $J.\ Phys.\ Sci\ 19,\ 51–59.$

Keshavarz, M., Shourijeh, P. T., and Hekmatzadeh, A. A. (2024). The erosion resistance of clay soil treated with recycled concrete aggregates. *Construction Building Materials* 443, 137733. doi: 10.1016/J.CONBUILDMAT.2024.137733

Kirwan, M. L., and Megonigal, J. P. (2013). Tidal wetland stability in the face of human impacts and sea-level rise. *Nature* 504, 53–60. doi: 10.1038/nature12856

Le Hir, P., Roberts, W., Cazaillet, O., Christie, M., Bassoullet, P., and Bacher, C. (2000). Characterization of intertidal at hydrodynamics. *Continental Shelf Res.* 20, 1433–1459. doi: 10.1016/S0278-4343(00)00031-5

Leonardi, N., Ganju, N. K., and Fagherazzi, S. (2016). A linear relationship between wave power and erosion determines salt-marsh resilience to violent storms and hurricanes. *Proc. Natl. Acad. Sci. United States America* 113, 64–68. doi: 10.1073/pnas.1510095112

Li, Z., Dong, S., Ashour, A., al, -, Hannanee Ahmad Zaidi, F., Ahmad, R., et al. (2021). A review of concrete durability in marine environment. *IOP Conf. Series: Materials Sci Eng.* 1175, 12018. doi: 10.1088/1757-899X/1175/1/012018

Lick, W., and McNeil, J. (2001). Effects of sediment bulk properties on erosion rates. Sci Total Environ, 266, 41–48, doi: 10.1016/S0048-9697(00)00747-6

Loke, L. H. L., Bouma, T. J., and Todd, P. A. (2017). The effects of manipulating microhabitat size and variability on tropical seawall biodiversity: field and flume experiments. *J. Exp. Mar. Biol. Ecol.* 492, 113–120. doi: 10.1016/j.jembe.2017.01.024

Loke, L. H. L., Bouma, T. J., and Todd, P. A. (2015). Creating complex habitats for restoration and reconciliation. *Ecol. Eng.* 77, 307–313. doi: 10.1016/j.ecoleng.2015.01.037

Ma, D., Zhang, M., and Cui, J. (2023). A review on the deterioration of mechanical and durability performance of marine-concrete under the scouring action. *J. Building Eng.* 66, 105924. doi: 10.1016/J.JOBE.2023.105924

Marin-Diaz, B., Fivash, G. S., Nauta, J., Temmink, R. J. M., Hijner, N., Reijers, V. C., et al. (2021). On the use of large-scale biodegradable artificial reefs for intertidal foreshore stabilization. *Ecol. Eng.* 170, 106354. doi: 10.1016/J.ECOLENG.2021.106354

Marin-Diaz, B., Govers, L. L., van der Wal, D., Olff, H., and Bouma, T. J.. (2022). The importance of marshes providing soil stabilization to resist fast-flow erosion in case of a dike breach. *Ecol. Appl.* 32, 1–16. doi: 10.1002/eap.2622

Marin-Diaz, B., van der Wal, D., Kaptein, L., Martinez-Garcia, P., Lashley, C. H., de Jong, K., et al. (2023). Using salt marshes for coastal protection: Effective but hard to get where needed most. *J. Appl. Ecol.* 60, 1286–1301. doi: 10.1111/1365-2664.14413

Mason, V. G., Burden, A., Epstein, G., Jupe, L. L., Wood, K. A., and Skov, M. W. (2023). Blue carbon benefits from global saltmarsh restoration. *Global Change Biol.* 29, 6517–6545. doi: 10.1111/gcb.16943

Möller, I., Kudella, M., Rupprecht, F., Spencer, T., Paul, M., van Wesenbeeck, B. K., et al. (2014). Wave attenuation over coastal salt marshes under storm surge conditions. *Nat. Geosci.* 7, 727–731. doi: 10.1038/ngeo2251

Morris, R. L., Bilkovic, D. M., Walles, B., and Strain, E. M. A. (2022). Nature-based coastal defence: Developing the knowledge needed for wider implementation of living shorelines. *Ecol. Eng.* 185, 106798. doi: 10.1016/J.ECOLENG.2022.106798

Mos, B., Dworjanyn, S. A., Mamo, L. T., and Kelaher, B. P. (2019). Building global change resilience: Concrete has the potential to ameliorate the negative effects of climate-driven ocean change on a newly-settled calcifying invertebrate. *Sci Total Environ*. 646, 1349–1358. doi: 10.1016/j.scitotenv.2018.07.379

Narayan, S., Beck, M. W., Reguero, B. G., Losada, I. J., van Wesenbeeck, B., Pontee, N., et al. (2016). The effectiveness, costs and coastal protection benefits of natural and nature-based defences. *PloS One* 11, e0154735. doi: 10.1371/JOURNAL.PONE.0154735

Natanzi, A. S., Thompson, B. J., Brooks, P. R., Crowe, T. P., and McNally, C. (2021). Influence of concrete properties on the initial biological colonisation of marine artificial structures. *Ecol. Eng.* 159, 106104. doi: 10.1016/j.ecoleng.2020.106104

Nitsch, C. K., Walters, L. J., Sacks, J. S., Sacks, P. E., and Chambers, L.G. (2021). Biodegradable material for oyster reef restoration: First-year performance and biogeochemical considerations in a coastal lagoon. *Sustainability (Switzerland)* 13, 7415. doi: 10.3390/su13137415

Nordstrom, K. F. (2014). Living with shore protection structures: A review. *Estuarine Coast. Shelf Sci* 150, 11–23. doi: 10.1016/J.ECSS.2013.11.003

Pan, Y., Tong, H., Wei, D., Xiao, W., and Xue, D. (2022). Review of structure types and new development prospects of artificial reefs in China. *Front. Mar. Sci* 9. doi: 10.3389/FMARS.2022.853452/XML

Peng, R., Qiu, W., and Teng, F. (2022). Investigation on seawater freeze-thaw damage deterioration of marine concrete structures in cold regions from multi-scale. *Ocean Eng.* 248, 110867. doi: 10.1016/j.oceaneng.2022.110867

Piazza, B. P., Banks, P. D., and La Peyre, M. K. (2005). The potential for created oyster shell reefs as a sustainable shoreline protection strategy in Louisiana. *Restor. Ecol.* 13, 499–506. doi: 10.1111/j.1526-100X.2005.00062.x

Polk, M. A., Gittman, R. K., Smith, C. S., and Eulie, D. O. (2022). Coastal resilience surges as living shorelines reduce lateral erosion of salt marshes. *Integrated Environ. Assess. Manage.* 18, 82–98. doi: 10.1002/ieam.4447

Reimann, L., Vafeidis, A. T., and Honsel, L. E. (2023). Population development as a driver of coastal risk: Current trends and future pathways. *Cambridge Prisms: Coast. Futures* 1, e14. doi: 10.1017/cft.2023.3

Ridge, J. T., Rodriguez, A. B., Fodrie, F. Joel, Lindquist, N. L., Brodeur, M. C., Coleman, S. E., et al. (2015). Maximizing oyster-reef growth supports green infrastructure with accelerating sea-level rise. *Sci. Rep.* 5, 1–8. doi: 10.1038/erp.14785

Riera, E., Mauroy, B., Francour, P., and Hubas, C. (2024). Establishing complexity targets to enhance artificial reef designs. *Sci. Rep.* 14, 22060. doi: 10.1038/s41598-024-7227-7

Rijn, L. C. v. (1993). Principles of sediment transport in rivers, estuaries, and coastal seas. Available online at: https://www.nhbs.com/principles-of-sediment-transport-in-rivers-estuaries-and-coastal-seas-2-volume-set-book (Accessed January 28, 2025).

Saintilan, N., Kovalenko, K. E., Guntenspergen, G., Rogers, K., Lynch, J. C., Cahoon, D. R., et al. (2022). Constraints on the adjustment of tidal marshes to accelerating sea level rise. *Science* 377, 523–527. doi: 10.1126/science.abo7872

Sakr, A., and Altieri, A. H. (2025). Living in a material world: Support for the use of natural and alternative materials in coastal restoration and living shorelines. *Ecol. Eng.* 211, 107462. doi: 10.1016/j.ecoleng.2024.107462

San Juan, J. E., Wei, W. G., and Yang, J. Q. (2024). Impact of salinity on the erosion threshold, yield stress, and gelatinous state of a cohesive clay. *J. Geophysical Research: Earth Surface* 129, e2023JF007485. doi: 10.1029/2023JF007485

Schoonees, T., Gijón Mancheño, A., Scheres, B., Bouma, T. J., Silva, R., Schlurmann, T., et al. (2019). Hard structures for coastal protection, towards greener designs. *Estuaries Coasts* 42, 1709–1729. doi: 10.1007/s12237-019-00551-z

Schotanus, J., Walles, B., Capelle, J. J., van Belzen, J., van de Koppel, J., and Bouma, T. J. (2020). Promoting self-facilitating feedback processes in coastal ecosystem engineers to increase restoration success: Testing engineering measures. *J. Appl. Ecol.* 57, 1958–1968. doi: 10.1111/1365-2664.13709

Setunge, S., Nguyen, N., Alexander, B. L., and Dutton, L. (2009). Leaching of alkali from concrete in contact with waterways. *Water Air Soil Pollution: Focus* 9, 381–391. doi: 10.1007/S11267-009-9234-X

Shepard, C. C., Crain, C. M., and Beck, M. W. (2011). The protective role of coastal marshes: A systematic review and meta-analysis. *PloS One* 6, e27374. doi: 10.1371/journal.pone.0027374

Smith, C. S., Rudd, M. E., Gittman, R. K., Melvin, E. C., Patterson, V. S., Renzi, J. J., et al. (2020). Coming to terms with living shorelines: A scoping review of novel restoration strategies for shoreline protection. *Front. Mar. Sci* 7. doi: 10.3389/fmars.2020.00434

Stoorvogel, M. M., Temmerman, S., Oosterlee, L., Schoutens, K., Maris, T., van de Koppel, J., et al. (2024). Nature-based shoreline protection in newly formed tidal marshes is controlled by tidal inundation and sedimentation rate. *Limnology Oceanography* 69, 2377–2390. doi: 10.1002/LNO.12676

Strain, E. M. A., Olabarria, C., Mayer-Pinto, M., Cumbo, V., Morris, R. L., Bugnot, A. B., et al. (2018). Eco-engineering urban infrastructure for marine and coastal biodiversity: Which interventions have the greatest ecological benefit? *J. Appl. Ecol.* 55, 426–441. doi: 10.1111/1365-2664.12961

Tamburri, M. N., Luckenbach, M. W., Breitburg, D. L., and Bonniwell, S. M. (2008). Settlement of Crassostrea ariakensis larvae: effects of substrate, biofilms, sediment and adult chemical cues. *J. Shellfish Res.* 27, 601–608. doi: 10.2983/0730-8000(2008)27[601: SOCALE]2.0.CO;2

Temmerman, S., Meire, P., Bouma, T. J., Herman, P. M. J., Ysebaert, T., and De Vriend, H. J. (2013). Ecosystem-based coastal defence in the face of global change. *Nature* 504, 79–83. doi: 10.1038/nature12859

Temmink, R. J. M., Angelini, C., Verkuijl, M., and van der Heide, T.. (2023). Restoration ecology meets design-engineering: Mimicking emergent traits to restore feedback-driven ecosystems. *Sci. Total Environ.* 902, 166460. doi: 10.1016/J.SCITOTENV.2023.166460

Theuerkauf, S. J., Burke, R., Burke, R. P., and Lipcius, R. N. (2015). Survival of eastern oysters on alternative reef substrates article. *J. Shellfish Res.* 34, 241–250. doi: 10.2983/35.034.0205

van de Koppel, J., van der Wal, D., Bakker, J. P., and Herman, P. M. J. (2005). Selforganization and vegetation collapse in salt marsh ecosystems. *Am. Nat.* 165, E1–12. doi: 10.1086/426602

Van der Wal, D., Wielemaker-Van den Dool, A., and Herman, P. M. J. (2008). Spatial patterns, rates and mechanisms of saltmarsh cycles (Westerschelde, The Netherlands). *Estuarine Coast. Shelf Sci* 76, 357–368. doi: 10.1016/j.ecss.2007.07.017

Van Loon-Steensma, J. M., and Slim, P. A. (2013). The impact of erosion protection by stone dams on salt-marsh vegetation on two wadden sea barrier islands. *J. Coast. Res.* 26, 783–796. doi: 10.2307/23486550

Van Loon-Steensma, J. M., and Vellinga, P. (2013). Trade-offs between biodiversity and flood protection services of coastal salt marshes. *Curr. Opin. Environ. Sustainability* 5, 320–326. doi: 10.1016/j.cosust.2013.07.007

Vuik, V., Jonkman, S. N., Borsje, B. W., and Suzuki, T. (2016). Nature-based flood protection: The efficiency of vegetated foreshores for reducing wave loads on coastal dikes. *Coast. Eng.* 116, 42–56. doi: 10.1016/j.coastaleng.2016.06.001

Walles, B., Troost, K., van den Ende, D., Nieuwhof, S., Smaal, A. C., and Ysebaert, T. (2016). From artificial structures to self-sustaining oyster reefs. *J. Sea Res.* 108, 1–9. doi: 10.1016/j.seares.2015.11.007

Wang, H., Long, G., Xie, Y., Zeng, X., Ma, K., Dong, R., et al. (2022). Effects of intense ultraviolet irradiation on drying shrinkage and microstructural characteristics of cement mortar. *Construction Building Materials* 347, 128513. doi: 10.1016/J.CONBUILDMAT.2022.128513

Wijsman, J. W. M., Foekema, E. M., and van den Heuvel-Greve, M. J. (2024). Uitloging LD-staalslakken: Overzicht bestaande kennis van de effecten bij toepassing in de Ooster- en Westerschelde. doi: 10.18174/657884

Zhang, Z., Niu, Y., Shang, X., Ye, P., Zhou, R., and Gao, F. (2021). Deterioration of physical and mechanical properties of rocks by cyclic drying and wetting. *Geofluids* 2021, 6661107. doi: 10.1155/2021/6661107

Zhu, Z., Vuik, V., Visser, P. J., Soens, T., van Wesenbeeck, B., van de Koppel, J., et al. (2020). Historic storms and the hidden value of coastal wetlands for nature-based flood defence. *Nat. Sustainability* 3, 853–862. doi: 10.1038/s41893-020-0556-z

Zimmermann, L., Dombrowski, A., Völker, C., and Wagner, M. (2020). Are bioplastics and plant-based materials safer than conventional plastics? *In vitro* toxicity and chemical composition. *Environ. Int.* 145, 106066. doi: 10.1016/j.envint.2020.106066